

REDESIGN OF THE GANIL GTS ECRIS FOR 1+/N+ STUDIES

V. Toivanen[†], P. Jardin, L. Maunoury, C. Michel
Grand Accélérateur National d'Ions Lourds (GANIL), F-14076 Caen Cedex 05, France

Abstract

More than half of the beams produced at GANIL are metallic elements, underlining the importance of their continuing development. Compared to the conventional techniques (oven, sputtering, MIVOC), the 1+/n+ method has demonstrated superior ionization efficiencies, suggesting the potential for improved metal beam production. Dedicated studies are required to assess the feasibility of this approach. The SPIRAL1 Charge Breeder is now in operation at the GANIL radioactive beam facility SPIRAL1. Operation in high radiation area poses challenges for its future development. A separate test stand supporting charge breeder and metal ion beam R&D is thus desirable.

The GTS 14.5 GHz ECRIS has been chosen as a platform for 1+/n+ studies. After the upgrade program of 2017-2018, the GTS provides good performance and versatility, making it well-suited for ion source R&D. A new injection module has been designed for 1+ injection into the GTS plasma to be used in the 1+/n+ studies. It can be easily replaced with the conventional system for normal ion source operation. The design of the new injection system will be presented in detail with ion optical simulations of the 1+ beam injection.

INTRODUCTION

The GTS 14.5 GHz Electron Cyclotron Resonance (ECR) ion source has undergone a substantial upgrade program in 2017 - 2018. As part of this upgrade, the ion source beam extraction system was refurbished, a new center coil was added to improve the magnetic field control and the injection side of the source was redesigned to reach higher injection magnetic fields and to allow double frequency operation in a wide frequency range. These changes are discussed in more detail in Ref. [1]. As presented there, the extraction system and center coil upgrades yielded an improvement of up to a factor of three for the delivered beam currents in 2017. In 2018 the new injection system has been commissioned for operation, which has provided further performance improvements, especially for the high charge state beams. For example, with double frequency operation (14.5 GHz + 11.215 GHz) the GTS has recently produced a 17.5 μA beam of $^{129}\text{Xe}^{30+}$, which is over eight times higher intensity than before the upgrade program.

The motivation for the GTS upgrades has been two-fold. First, the goal was to improve the beam capabilities available for the multidisciplinary low energy beam facility ARIBE (Accélérateurs pour les Recherches Interdisciplinaires avec les Ions de Basse Energie), which is the primary user of the GTS beams. The second goal was to establish a good baseline performance for continued ion source R&D with

the GTS. As these goals have now been achieved, the next phase for the GTS is to utilize it for charge breeding (or 1+/n+ method) research. This will be a second role for the GTS, as it will also continue to serve the ARIBE facility in its conventional ion source configuration.

One potential future application of the 1+/n+ method is enhanced metal ion production. Metal ion beams are currently widely used in the accelerator facilities around the world, and as an example, more than 50 % of the beams delivered at GANIL are metallic elements. This highlights the importance to continue metal ion production development with ECR ion sources. With conventional techniques like sputtering, miniature ovens and MIVOC, the global ionization efficiencies of metal beams is low. Here, the global efficiency is defined as the ratio of the extracted ion flow (all ion species of the element) over the injected neutral flow. Based on the data collected from GANIL operation, published in Ref. [2], the typical measured global efficiencies for sputtering are around 1 %, oven beams around 10 % and MIVOC beams around 20 %. In total, all measured efficiency data is below 30 %. In contrast, experience with charge breeders has shown that with 1+ injection global efficiencies around and in excess of 50 % are achievable (see e.g. Ref. [3]). The higher efficiency would first of all reduce the material consumption, which is not an insignificant consideration for rare and expensive elements and isotopes. Secondly, decrease in injected material would reduce the plasma chamber contamination. Furthermore, decoupling the initial metal ion production and the stepwise multi-ionization allows both of these processes to be optimized independently.

However, dedicated studies are necessary to validate the feasibility of these ideas. One of the main challenges that needs to be assessed is the high intensity operation. Although several measurements performed so far suggest a weak relationship between the 1+ capture and ionization efficiencies and the injected 1+ current, this effect has been mainly studied with low currents up to only a few μA (see e.g. Refs. [4–7]). In order to make 1+/n+ method a realistic alternative for the conventional techniques, it must be demonstrated that the high efficiencies can be retained also with significantly higher current levels. The GTS can provide a suitable test bench for these studies.

The GTS will be used also for studying other aspects of charge breeding. The SPIRAL1 Charge Breeder has been recently installed and commissioned at the GANIL radioactive ion beam facility SPIRAL1 [8]. The role of the machine is to charge breed the singly charged radioactive elements produced by the Target Ion Source Systems (TISS) and deliver the multiply charged ions for post-acceleration and experiments. As an operational machine in a high radiation dose area, the access to the charge breeder will be limited

[†] ville.toivanen@ganil.fr

Content from this work may be used under the terms of the CC BY 3.0 licence (© 2018). Any distribution of this work must maintain attribution to the author(s), title of the work, publisher, and DOI.

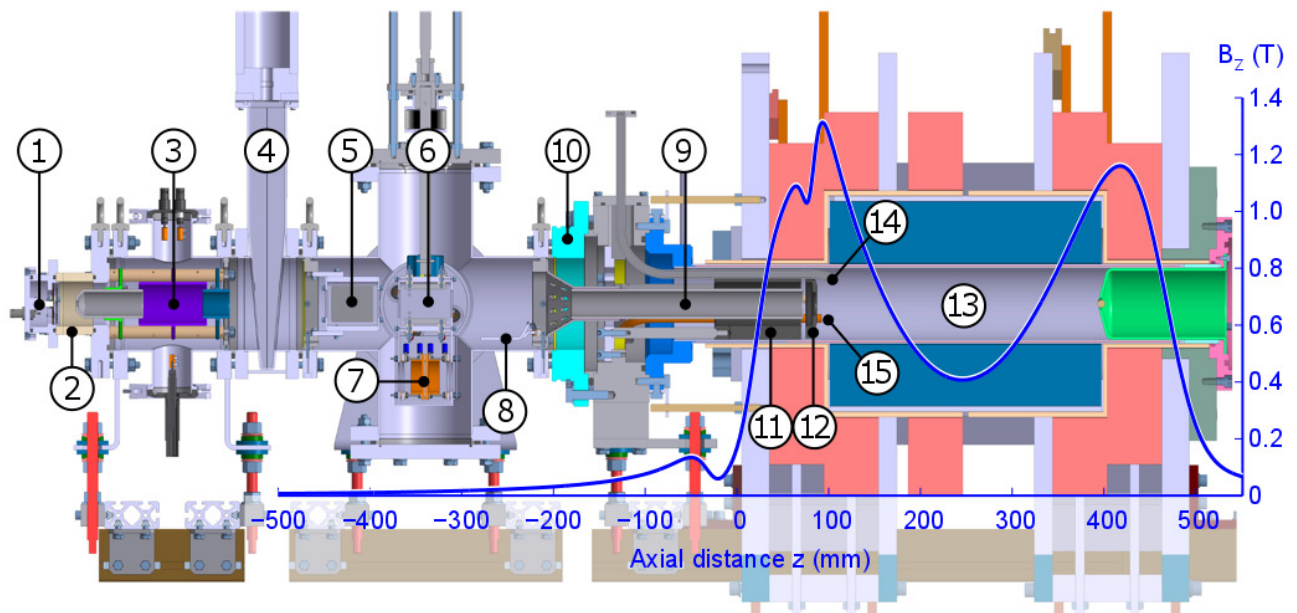


Figure 1: Cross section view of the 1+ beam injection module connected to the GTS. The main parts include (1) a 1+ source, (2) an insulator, (3) a 1+ beam extraction system (a puller electrode and an einzel lens), (4) an isolating valve, (5) horizontal and (6) vertical steerers, (7) two-sided Faraday cup, (8) a beam dump, (9) a grounded guiding tube, (10) a main insulator, (11) an ARMCO cylinder, (12) an ARMCO injection aperture electrode (IAE), (13) the GTS plasma chamber, (14) a WR62 waveguide and (15) a gas injection tube. The second WRD750 wave guide is not visible in this view. The GTS axial magnetic field is also presented.

in the future, which will set restrictions to its development. As such, it will be beneficial to have access to an offline test bench to perform charge breeder specific R&D. The operational experience and mechanical upgrades developed with the test bench can then be transferred to the SPIRAL1 Charge Breeder.

In order to use the GTS for the charge breeding (1+/n+ method) studies, it needs to be modified to allow 1+ beam injection into the ECR plasma. These modifications are presented in the following chapter.

INJECTION MODULE DESIGN

One of the main principles of the GTS modifications is the ability to transition from normal ion source operation to 1+/n+ operation (and vice versa) in a relatively short time. To accommodate this requirement, a new injection side module has been designed which completely replaces the conventional ECRIS injection system hardware when the GTS will be operated with 1+ beam injection. The existing injection system can be pulled out of the ion source on rails and lifted off as a single unit. The dedicated 1+ injection hardware can then be lifted on the rails and connected to the ion source. Including the pumping time, a beam-to-beam time of a few days should be realistic with this approach when the GTS is transitioned between conventional ion source operation and 1+/n+ studies.

The design of the 1+ injection module is presented in Fig. 1. The 1+/n+ studies will start using an existing alkali ion source as the source of singly charged ions. It is based on

thermal ion emission from a heated porous tungsten pellet that is doped with the alkali element of interest. Based on past experience, the source can deliver 1+ ions from nA levels up to around 1 mA, offering a wide current range for experiments. The 1+ source is electrically separated from the rest of the system, and it will be operated at a potential of $V_{1+} = V_{GTS} + \Delta V$, where V_{GTS} is the potential of the GTS plasma chamber and ΔV is an adjustable voltage to allow the ions to overcome the positive plasma potential to enter the GTS plasma volume. The transport section between the 1+ source and the GTS plasma chamber is grounded, so the ion kinetic energy in this region is $e(V_{GTS} + \Delta V)$.

The 1+ source features a Wehnelt electrode to control the beam formation from the heated pellet. Normally the Wehnelt is biased negatively to some hundreds of Volts with respect to the pellet potential. The 1+ source is followed by a beam extraction system consisting of a puller electrode and a positive (decelerating) einzel lens. The pellet source and the extraction system can be separated from the rest of the injection module with a gate valve. This allows manipulation and exchange of the 1+ source without compromising the GTS vacuum.

The design features two independent steerers (horizontal and vertical) which can be used to manipulate the beam as it passes through the injection system. With low steerer voltages the beam alignment with respect to the optical axis can be varied. This can be used to correct beam misalignments or to study the effects of varying the transverse insertion location of the beam into the GTS plasma chamber. The ver-

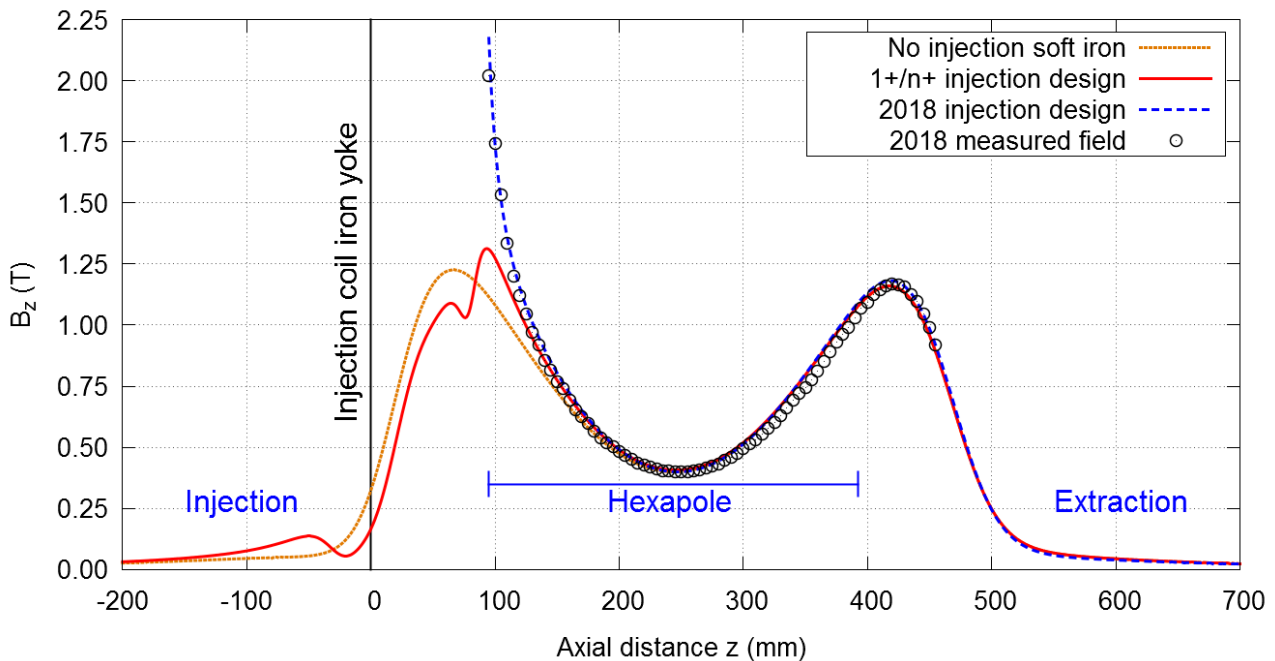


Figure 2: GTS axial field profile with different injection soft iron configurations. The 2018 design corresponds to the new injection system installed in 2018 for conventional ion source operation. In all cases the injection, center and extraction coil currents are 1200 A, 0 A and 1100 A, respectively.

tical steerer is designed to be used also for beam pulsing. In this operation mode the 1+ beam is deviated into a dedicated beam dump. In principle any desired pulse pattern can be created for the of 1+ beam by varying the vertical steerer potential as a function of time. This feature is especially important for the studies involving measurements of charge breeding time.

After the steerers the beam enters a grounded tube that guides the ions inside the GTS high voltage enclosure. The 1+ ions are decelerated into the GTS plasma volume between the end of the grounded tube and a conically shaped injection aperture electrode (see (12) in Fig. 1). The injection aperture electrode can be biased with respect to the plasma chamber potential. In this configuration it can be used in a similar fashion as the biased disc of a conventional ECR ion source. However, as the electrode is situated only around the axis, experimental work is required to determine its effectiveness in 1+/n+ operation.

For beam diagnostics the injection design features a two-sided Faraday cup, which can be moved on an actuator to replace the vertical steerer. The Faraday cup can be used to measure both the 1+ beam current from the 1+ source as well as the beam current of the ions extracted from the GTS plasma chamber towards the injection. In addition, the current collected on the beam dump and on the grounded guiding tube can be measured.

The injection design features two wave guides for microwave injection; a WR62 for nominal 14.5 GHz operation and a double-ridge WRD750 with a wide 8 – 18 GHz range for varied or double frequency operation. Gas injection is

performed through a dedicated gas tube. Due to the Halbach-style hexapole, access through the injection is the only option for microwave and gas insertion. The wave guides and the gas pipe enter the GTS plasma chamber through the edges of the injection aperture electrode with a 120° azimuthal symmetry. This is done to ensure symmetrical cuts on the soft iron pieces to minimize asymmetry in the injection magnetic field. Field asymmetry in this region can lead to unwanted steering of the incoming ions, degrading the injection efficiency [3, 6, 9]. In addition, this solution places the wave guides and the gas pipe between the arms of the star-shaped axial plasma loss pattern.

To allow access for the 1+ beam, the solid soft iron plug that boosts the injection axial magnetic field in conventional ECRIS configuration is not possible in the 1+/n+ operation mode. This unavoidably leads to decreased magnetic field in this region. However, the removal of the injection plug is partly compensated with a new soft iron structure around the space that is required for the beam injection.

The magnetic design calculations were performed with the Radia software [10]. After studying several geometrical options within the boundary conditions set by the GTS structure, a design featuring a hollow ARMCO cylinder located around the grounded tube and a conical ARMCO tip with a smaller 25 mm aperture was chosen (parts (11) and (12) in Fig. 1). The conical piece also fulfills the role of the injection aperture electrode discussed previously. The chosen design provides a 1.32 T axial field maximum, which is located at the injection end of the GTS hexapole magnet. This value is comparable with the injection field of the SPI-

Content from this work may be used under the terms of the CC BY 3.0 licence (© 2018). Any distribution of this work must maintain attribution to the author(s), title of the work, publisher, and DOI.

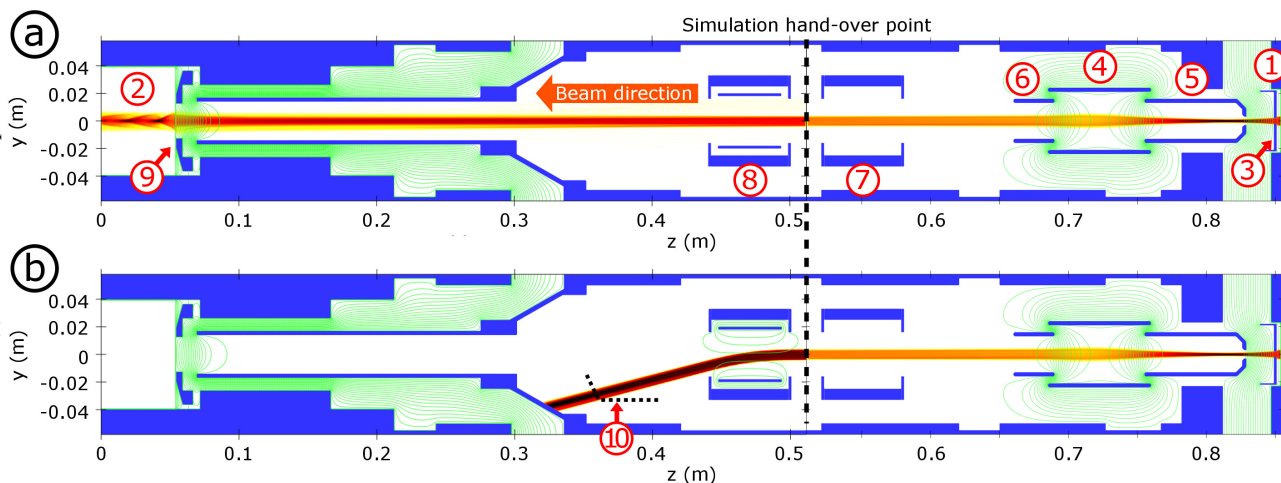


Figure 3: *Case (a)*: Ion optical simulation (trajectory density) for $10 \mu\text{A}$ of $^{39}\text{K}^+$ ions extracted from the 1+ source (1), transported through the injection module and decelerated into the GTS plasma chamber (2). Plasma potential is 10 V. The 1+ source potential is $V_{1+} = V_{GTS} + \Delta V$, where $V_{GTS} = 15 \text{ kV}$ and $\Delta V = 30 \text{ V}$. The 1+ source Wehnelt electrode (3) is at $V_W = V_{1+} - 600 \text{ V}$ and the einzel electrode (4) at 11 kV. The puller (5) and the last extraction electrode (6) are grounded. Both steerers (7 and 8) are off, i.e. grounded. The injection aperture electrode (IAE) (9) is at GTS chamber potential; $V_{IAE} = V_{GTS} = 15 \text{ kV}$. The 1+ beam transmission from the 1+ source to inside the GTS plasma chamber is 92 %. *Case (b)*: An example of beam deflection with the vertical steerer for pulsed 1+ beam operation. The steerer plates are set to $\pm 3 \text{ keV}$. The location of the beam dump (10) is presented with a dashed line.

RAL1 Charge Breeder and is close to the 1.4 T value of the ECR Charge Breeder at ANL [9], which further increases the confidence to the design. The calculated axial magnetic field is presented in Fig. 2, compared to the current GTS axial field in conventional ion source operation mode. A case without any added soft iron in the injection side of the GTS is also shown. The measured field values with the current injection system are also included, demonstrating the good correlation between the field calculated with the Radia model and the reality. In Fig. 1 the axial field is overlaid with the mechanical design of the injection module and the GTS.

ION OPTICAL SIMULATIONS

The injection module design was developed with the aid of ion optical simulations. The simulations were performed with the code IBSimu [11], utilizing the 3D magnetic field maps calculated for the system with Radia. The simulation model includes the magnetic field present inside the ion source as well as the fringe field that extends into the injection module region. The field map contains both the solenoid and the hexapole field components of the ion source.

A simplified plasma volume is implemented in the simulation model to approximate the influence of the plasma to the 1+ ion trajectories at the entrance to the GTS plasma chamber. The plasma volume is modeled with an analytical electron background which compensates the ion space charge. A constant plasma potential of 10 V is imposed inside the plasma volume and its boundaries are kept constant, as the plasma is assumed not to be significantly influenced by the injected 1+ ions. The axial boundary is set at the

plasma facing surface of the injection aperture electrode. Collisions between injected 1+ ions and plasma particles are not included in the simulation model.

In order to keep the simulation volume at a manageable size and to reduce the system memory requirements, the simulations were performed in two parts. The system is divided in the axial direction with the hand-over point at $z = 0.511 \text{ m}$ in simulation coordinates (see Fig. 3). This location was chosen as it provides a potential free region and thus omitting the geometry on one side of this position does not influence the ion behavior.

The main baseline beam used in the simulations is $^{39}\text{K}^+$, extracted from the 1+ source with voltages around 15 kV. An example of $^{39}\text{K}^+$ injection into the GTS plasma chamber is presented in Fig. 3(a). The extracted beam current is $10 \mu\text{A}$ and the 4rms-emittance is 20 mm mrad. The relevant potential values are presented in the figure caption. It is observed that the einzel lens provides a small diameter parallel beam through the injection module. 100 % of the 1+ beam is transported through the module and the beam enters the plasma chamber on the optical axis of the system. The beam is decelerated in a controlled manner, though some particle losses are observed here due to ions being reflected back by the plasma potential. This process is mainly dictated by the magnitude of the ion velocity component perpendicular to the plasma sheath with respect to the plasma potential value. In the presented case with $\Delta V = 30 \text{ V}$ the transmission from the 1+ source to the inside of the GTS plasma chamber is about 92 %. However, it is pointed out that these transmission numbers should be taken only as guiding values, as in reality the ion motion in this region is influenced by the

presence of the plasma particles (collisions, thermalisation, diffusion and ions extracted towards injection), which are not included in the current model. Inside the plasma chamber the magnetic field of the GTS has a strong influence on the low energy ions, forcing them into a corkscrew motion.

The effect of varying the bias voltage of the injection aperture electrode ((9) in Fig. 3) was studied with simulations. The bias voltage was varied between 0 V and -500 V with respect to the plasma chamber potential. Based on the simulations the influence of the varied bias on the 1+ beam transmission into the GTS plasma chamber is negligible (< 0.5 %-point). This suggests that the bias can be tuned to optimize plasma processes without compromising the ion injection efficiency.

The vertical steerer is designed to be used for beam pulsing. A simulation demonstrating the redirection of the 1+ beam into the dedicated beam dump is presented in Fig. 3(b).

One of the potential sources of issues with 1+/n+ operation is the ion beam extracted from the GTS plasma chamber towards the injection and the 1+ source. The aperture that allows the injection of 1+ beam into the plasma chamber also unavoidably acts as an extraction channel for the plasma ions. If high amounts of ions are extracted from the plasma through the grounded guiding tube, it could have adverse effects on the operation of the injection module and the 1+ source. In order to study this scenario with simulations, the GTS plasma chamber was populated with oxygen ions and 0.9 mA of ionic current was extracted towards the injection. The oxygen ion population consisted of charge states ranging from 1+ to 8+ following the shape of a typical oxygen charge state distribution produced with the GTS, peaking at the $^{16}\text{O}^{6+}$. Based on the simulations over 90 % of the ions escaping from the plasma chamber are lost inside the grounded tube and only 0.6 % of them reach the 1+ source, amounting to about 5.4 μA in this case. These surviving ions are almost exclusively collected on the Wehnelt electrode, for which this level of additional current will not cause any issues. Similarly, the grounded outer bodies of the steerers will collect a few tens of μA of current, as well as the last grounded electrode of the einzel lens assembly. Based on these results it is not expected that these ions will cause any significant issues for the operation of the 1+ injection module.

CONCLUSIONS

Due to its diverse features, the presented injection module design demonstrates a good potential for 1+/n+ operation

and the related studies. The similarities in the injection magnetic field between the GTS and the SPIRAL1 Charge Breeder and the results of the ion optical simulations give confidence for the design choices. The ion deceleration and insertion into the ECR plasma is a critical part of the system, and the most challenging to model reliably. This is taken into account in the mechanical details of the design to make it easier to vary the system geometry in this location (e.g. the grounded tube dimensions and position, replacement of the injection aperture electrode). This gives flexibility for geometry optimization, as the operational experience with the system increases.

The installation of the injection module and the first measurements with the GTS in 1+/n+ operation mode are expected to take place in 2019. The experiments will start with the existing alkali source to produce the 1+ ions. As the features of this source are well known, it is well suited for the commissioning of the 1+ injection system and its features. The GTS performance can also be benchmarked and compared to the SPIRAL1 Charge Breeder, which has been operated with the same 1+ source. Later the alkali source can be replaced with other 1+ sources to expand the studies to other elements.

REFERENCES

- [1] V. Toivanen *et al.*, in *Proc. of ICIS'17*, Geneva, Switzerland (2017), to be published in the AIP Conference Proceedinds.
- [2] C. Barué *et al.*, in *Proc. of ECRIS'16*, Busan, Korea (2016).
- [3] R. Vondrasek *et al.*, *Rev. Sci. Instrum.*, vol. 82, p. 053301 (2011).
- [4] L. Maunoury *et al.*, *Rev. Sci. Instrum.*, vol. 85, p. 02A504 (2014).
- [5] L. Maunoury *et al.*, in *Proc. of ECRIS'16*, Busan, Korea (2016).
- [6] T. Lamy *et al.*, in *Proc. of ECRIS'14*, Nizhny Novgorod, Russia (2014).
- [7] H. Koivisto *et al.*, *Rev. Sci. Instrum.*, vol. 85, p. 02B917 (2014).
- [8] L. Maunoury *et al.*, in these proceedings.
- [9] R. Vondrasek *et al.*, *Rev. Sci. Instrum.*, vol. 85, p. 02B903 (2014).
- [10] RADIA magnetic field simulation code, <http://www.esrf.eu/Accelerators/Groups/InsertionDevices/Software/Radia>.
- [11] T. Kalvas *et al.*, *Rev. Sci. Instrum.*, vol. 81, p. 02B703 (2010).